D. Large Lattice Distortion, Weak Coupling

Here the phonon solutions are strongly altered near the defect and there is the possibility of localized modes with a sharp frequency outside the bands and of scattering resonances with strongly increased local amplitudes. Thus, electronic transitions of proper symmetry types can couple to narrow frequency regions. But because of the weak coupling we may expect only a limited line structure above the zero-phonon line.

On the other hand, some cases such as M and R centers[22] and NO_2^- molecules[23] in alkali halides, as well as the $4f^n \rightarrow 4f^n$ transitions of Sm^{2+} in the alkali halides are not as easily classified. These defects are complex and should cause considerable local distortion. They should belong to either the case B or D. Yet the vibronic structures in parts of their spectra appear to represent coupling to certain singular points in the phonon distribution. It is possible that in these cases coupling to localized vibrations is forbidden by symmetry considerations. We intend to subject these cases to further study.

[22] D. B. Fitchen, R. H. Silsbee, T. A. Fulton, and E. L. Wolf, Phys. Rev. Letters **11**, 275 (1963).
[23] T. Timusk and W. Staude, Phys. Rev. Letters **13**, 373 (1964).

ACKNOWLEDGMENTS

The authors are indebted to a number of their colleagues for many useful discussions. Principally among these are Dr. W. R. Heller, Dr. J. D. Axe, and Dr. J. C. Slonczewski. The authors are also indebted to E. Bacanskas for his help in obtaining a part of the experimental data.

PHYSICAL REVIEW VOLUME 139, NUMBER 1A 5 JULY 1965

Paramagnetic Relaxation of Some Rare-Earth Ions in Diamagnetic Crystals*

CHAO-YUAN HUANG†
Division of Engineering and Applied Physics, Harvard University, Cambridge, Massachusetts
(Received 2 November 1964; revised manuscript received 17 February 1965)

The pulsed-saturation method at 8.9 kMc/sec was used to measure the spin-lattice relaxation rate T_1^{-1} for Eu^{2+}, Ho^{2+}, and Tm^{2+} in CaF_2, for Yb^{3+} in yttrium gallium garnet, yttrium aluminum garnet, and lutetium gallium garnet; for Nd^{3+} in yttrium gallium garnet and yttrium aluminum garnet; and for Sm^{3+} in lanthanum ethyl sulphate at low temperatures. The experimental data in most cases are in satisfactory agreement with the theoretical predictions based on the combined Van Vleck–Orbach theory. Besides the expected conventional processes, a process $T_1^{-1} \propto T^5$ was observed for Eu^{2+} in CaF_2 in the temperature range $15°K < 30°K$. Furthermore, a pronounced anisotropy in T_1 (a factor ~ 6) for Sm^{3+} in lanthanum ethyl sulphate was found both experimentally and theoretically.

I. INTRODUCTION

IT has been shown by Heitler and Teller,[1] Fierz,[2] Kronig,[3] Van Vleck[4] and others that the dominant spin-lattice interaction is through the thermal modulation of the Stark field. According to them the energy transfer between the spin system and the lattice vibration gives rise to two processes: (1) a one-phonon process in which a phonon is absorbed or emitted accompanied by a quantum jump of a spin between two Zeeman levels; (2) a two-phonon process in which a phonon is scattered by a spin and another phonon with different energy is emitted accompanied by a quantum jump of spin. Theoretically, it is found that the former predominates at low temperatures.

Before 1961, no detailed theory for the rare earths had existed. This problem was first attacked by Orbach[5] who uses a simple orbit-lattice interaction to estimate the spin-lattice relaxation time.

Since the divalent rare-earth ion in CaF_2 is surrounded by eight F ions sitting at the eight corners of a cube and the trivalent rare-earth ion in the garnet occupies the site surrounded by eight oxygen ions situated at the corners of a distorted cube,[6] the orbit-lattice interaction for an XY_8 molecular cluster is computed in Sec. II, based on the normal coordinates calculated by Huang and Inoue.[7] In order to facilitate the calculation of the spin-lattice relaxation time for Sm^{3+} in lanthanum ethyl sulphate, denoted LES, Orbach's phenomenological orbit-lattice interaction is criticized and improved. The formulas for calculating the spin-lattice relaxation times are also given in this section. The experimental results

* This work is supported by NONR 1866(16)7376-4.
† Present address: Research Institute for Advanced Studies, Baltimore, Maryland.
[1] W. Heitler and E. Teller, Proc. Roy. Soc. (London) **A155**, 629 (1936).
[2] M. Fierz, Physica **5**, 433 (1938).
[3] R. de L. Kronig, Physica **6**, 33 (1939).
[4] J. H. Van Vleck, Phys. Rev. **57**, 426 (1940).
[5] R. Orbach, Proc. Roy. Soc. (London) **A264**, 458 (1961).
[6] S. Geller and M. A. Gilleo, Acta. Cryst. **10**, 787 (1957).
[7] C. Y. Huang and M. Inoue, J. Phys. Chem. Solids **25**, 889 (1964).

along with the theoretical estimates are explicitly given in Sec. III.

II. THE ORBIT-LATTICE INTERACTION OF A MOLECULAR CLUSTER XY_8, COMPARISON WITH XY_6, AND FORMULAS OF T_1

1. Orbit-Lattice Interaction of a Molecular Cluster XY_8

The vibrations of an XY_8 molecular cluster transform according to the following irreducible representations of the O_h group, in Bethe's notations:

$$\Gamma(O_h^5)_{\text{vib}}=\Gamma_{1g}+\Gamma_{3g}+2\Gamma_{5g}+\Gamma_{2u}+\Gamma_{3u}+2\Gamma_{4u}+\Gamma_{5u}. \quad (1)$$

It will be seen later that only the normal coordinates of the even vibrations calculated by Huang and Inoue[6] need be considered.

According to Van Vleck,[4] the normal coordinates Q can be regarded as linear functions of the normal coordinates q_i associated with the phonons so that

$$Q_j=\sum_{i=1}^{3N} a_{ji}q_i, \quad (2)$$

where N is the total number of atoms in the entire crystal. Note the fact that the displacements of the lth corner atom (X_l,Y_l,Z_l) depend on any given thermal mode i of the vibration in the running wave form

$$X_l=q_i\Phi_{xi}\cos(\gamma_{li}-\delta_i), \quad (3)$$

$$\gamma_{li}=2\pi k_i(\lambda_{xi}x_l^0+\lambda_{yi}y_l^0+\lambda_{zi}z_l^0), \quad (4)$$

where Φ_{xi}, etc., are the direction cosines of the amplitude of the wave q_i, while k_i and λ_{xi}, etc., are, respectively, its wave vector and the direction cosines specifying its direction of polarization. x_l^0, etc., are the equilibrium coordinates of the lth corner atom. We suppose that the wavelength of the lattice vibration is long compared with the size of the molecular cluster so that we can take

$$\cos(\gamma_{li}-\delta_i)\simeq\cos\delta_i+\gamma_{li}\sin\delta_i. \quad (5)$$

Hence,

$$\begin{aligned}
a_{2i}&=U(-2\lambda_{xi}\Phi_{xi}+2\lambda_{yi}\Phi_{yi}),\\
a_{3i}&=U(-2\lambda_{xi}\Phi_{xi}-2\lambda_{yi}\Phi_{yi}+4\lambda_{zi}\Phi_{zi}),\\
a_{4i}&=U(-2\lambda_{yi}\Phi_{xi}-2\lambda_{xi}\Phi_{yi}),\\
a_{5i}&=U(-2\lambda_{zi}\Phi_{xi}-2\lambda_{xi}\Phi_{zi}),\\
a_{6i}&=U(-2\lambda_{zi}\Phi_{yi}-2\lambda_{yi}\Phi_{zi}),\\
a_{7i}&=a_{8i}=a_{9i}=0,
\end{aligned} \quad (6)$$

in which

$$U=2\pi Rk_i\sin\delta_i, \quad (7)$$

where $2R$ is the length of an edge of the cubic cluster.

Of the various forms of the orbit-lattice interaction that have been introduced, Van Vleck's[4] is the best. His method is used here. If the corner atoms can be regarded as isotropic, the mutual energy depends on distance only and the potential of the bonding electrons of the central atom due to the corner atoms is

$$V=\sum_0\sum_{i=1}^{8} f(r_{0i}), \quad (8)$$

where $\sum_0$ is the sum over all the bonding electrons of the central atom, r_{0i} is the distance between ith corner atom and an f electron of the central atom. Since only the symmetrical modes mainly contribute to relaxation,[4] the orbit-lattice interaction is written as

$$V_{01}=\sum_{j=2}^{9} v_jQ_j, \quad (9)$$

where v_j are the electronic operators and Q_j are as defined by Huang and Inoue.[6] v_j are obtained by expanding in terms of the electronic coordinates $(x_0y_0z_0)$ to sixth order

$$\begin{aligned}
v_2&=\sum_0\{A(x_0^2-y_0^2)+B(x_0^2-y_0^2)z_0^2+C[x_0^2y_0^2(x_0^2-y_0^2)+z_0^2(x_0^4-y_0^4)]+\cdots\},\\
v_3&=\sum_0\{A(x_0^2+y_0^2-2z_0^2)+B(2x_0^2y_0^2-z_0^2x_0^2-y_0^2z_0^2)\\
&\qquad +C(x_0^4y_0^2+z_0^2x_0^4+x_0^2y_0^4+y_0^4z_0^2+z_0^4x_0^2-2y_0^2z_0^4)+\cdots\}/(3)^{1/2},\\
v_4&=\sum_0\{Dx_0y_0+Ex_0y_0z_0^2+F[x_0^3y_0^3+3x_0y_0(x_0^2+y_0^2)z_0^2]+\cdots\},\\
v_5&=\sum_0\{Dz_0x_0+Ez_0x_0y_0^2+F[z_0^3x_0^3+3z_0x_0(x_0^2+z_0^2)y_0^2]+\cdots\},\\
v_6&=\sum_0\{Dy_0z_0+Ey_0z_0x_0^2+F[y_0^3z_0^3+3y_0z_0(y_0^2+z_0^2)x_0^2]+\cdots\},\\
v_7&=\sum_0\{Hy_0z_0+Iy_0z_0x_0^2+J[y_0^3z_0^3+3y_0z_0(y_0^2+z_0^2)x_0^2]+\cdots\},\\
v_8&=\sum_0\{Hz_0x_0+Iz_0x_0y_0^2+J[z_0^3x_0^3+3z_0x_0(z_0^2+x_0^2)y_0^2]+\cdots\},\\
v_9&=\sum_0\{Hx_0y_0+Ix_0y_0z_0^2+J[x_0^3y_0^3+3x_0y_0(x_0^2+y_0^2)z_0^2]+\cdots\},
\end{aligned} \quad (10)$$

in which

$$
\begin{aligned}
A&=2ee'(1-5r_0^2/27R^2-7r_0^4/54R^4)/(3)^{3/2}R^4,\\
B&=2ee'(35-14r_0^2/R^2)/81(3)^{1/2}R^6,\\
C&=77ee'/81(3)^{1/2}R^8,\\
D&=2ee'(-4/3+25r_0^2/27R^2+28r_0^4/81R^4)/(3)^{3/2}R^4,\\
E&=2ee'(-175/27+112r_0^2/81R^2)/(3)^{3/2}R^6,\\
F&=2ee'(3388/486)/(3)^{3/2}R^6,\\
H&=8ee'(5/3-91r_0^4/162R^4)/(3)^{3/2}R^4,\\
I&=392ee'r_0^2/243(3)^{1/2}R^8,\\
J&=4004ee'/729(3)^{1/2}R^8,
\end{aligned}
\tag{11}
$$

where e' is the effective charge of a corner ion. (v_5,v_6) and (v_8,v_9) can be obtained by, respectively, permuting v_4 and v_7 with respect to (x,y,z).

2. Comparison With XY_6

For an XY_6 molecular cluster, Van Vleck found[8]

$$v_2'=\sum_0\{A'(x_0^2-y_0^2)+B'(x_0^4-y_0^4)+\cdots\}, \tag{12}$$

which transforms according to the irreducible representation Γ_{3g} of the vibration, where

$$
\begin{aligned}
A'&=ee'\tfrac{1}{4}(18R'^4-75r_0^2/R'^6),\\
B'&=175ee'/8R'^6,
\end{aligned}
\tag{13}
$$

in which R' is the distance between the central ion X and the surrounding ions Y. He also found[4]

$$a_{2i}'=U'(\lambda_{xi}\Phi_{xi}-\lambda_{yi}\Phi_{yi}),$$

where

$$U'=2\pi R'k_i\sin\delta_i.$$

If we keep the distances between the X ion and the Y ions the same for both XY_6 and XY_8 and assume $\langle r_0^2\rangle\ll R^2$, then

$$Aa_{2i}/A'a_{2i}'=8/9 \tag{14}$$

and

$$Ba_{2i}/B'a_{2i}'=32/45. \tag{15}$$

Hence, the orbit-lattice interaction for an XY_8 molecular cluster is, in general, weaker than that of an XY_6 molecular cluster. However, we may still draw the conclusion that the orbit-lattice interaction is not very sensitive with respect to deviations from cubic symmetry.

3. Comments on Orbach's Phenomenological Orbit-Lattice Interaction

Orbach[5] has proposed an orbit-lattice interaction which was designed to yield estimates of the transition rate to within an order of magnitude or better and it is this procedure that we will briefly review here and comment upon.

[8] J. H. Van Vleck, J. Chem. Phys. **7**, 72 (1939).

One can write the static crystal-field interaction for the rare-earth ion as an expansion in normalized spherical harmonics

$$V_c=\sum_{n,m}V_n^m=\sum_{n,m}A_n^m\langle r_0^n\rangle Y_n^m(\theta,\phi). \tag{16}$$

Now the orbit-lattice interaction is just the thermal fluctuation in V_c. If ξ represents the coordinate of a surrounding atom, one can expand $A_n^m(\xi)$ in a Taylor's series about the equilibrium coordinate ξ_0,

$$A_n^m(\xi)=A_n^m(\xi_0)+\epsilon_{nm}\xi(\partial A_n^m/\partial\xi)_0+\cdots, \tag{17}$$

where ϵ_{nm} is the thermal lattice strain referring to that linear combination of suitable averaged components of the strain tensor which is appropriate to V_n^m. Then the Orbach's orbit-lattice interaction is expressed as

$$(V_{01})_0=\sum_{n,m}\epsilon_{nm}\left(\xi\frac{\partial A_n^m}{\partial\xi}\right)_0\langle r_0^n\rangle Y_n^m(\theta,\phi). \tag{18}$$

Orbach made the approximation that

$$|(\xi\partial A_n^m/\partial\xi)_0|\approx|A_n^m(\xi_0)|. \tag{19}$$

The last equation means that the dynamic crystal field interaction is approximately equal to the static one which is usually known experimentally. Thus,

$$(V_{01})_0=\sum_{n,m}\epsilon_{nm}A_n^m\langle r_0^n\rangle Y_n^m(\theta,\phi). \tag{20}$$

Actually, the relation given in Eq. (20) is a bad approximation. If a point-charge model is used, A_2^m is proportional to ξ^{-3}, A_4^m to ξ^{-5}, and A_6^m to ξ^{-6}. Hence,

$$|[\xi(\partial A_n^m/\partial\xi)]_0|=p_n|A_n^m(\xi_0)|, \tag{21}$$

where $p_n=3$, 5, 7 for $n=2$, 4, 6, respectively. The error involved in taking $p_n=1$ is very serious because the spin-lattice relaxation time calculated by the Orbach's method is no longer accurate within an order of magnitude. Especially for the case where $n=6$ terms are dominant, the relaxation rate for a two-phonon Raman process will be off by up to three orders of magnitude.

In order to get the crystalline field parameters which cannot be obtained from the experimental data, Orbach put

$$A_n^m\langle r_0^n\rangle=A_n^0\langle r_0^n\rangle, \tag{22a}$$

when $n=2$ or 4, and

$$A_6^m\langle r_0^6\rangle=[|A_6^0\langle r_0^6\rangle|^{6-|m|}|A_6^6\langle r_0^6\rangle|^{|m|}]^{1/6}. \tag{22b}$$

This was based on his satisfactory calculation of phonon anharmonic coefficients in dielectric crystals. It is well known that for a crystal in which the paramagnetic ions sit at the cubic sites, the only crystalline field parameters possibly obtained are $A_4^0\langle r_0^4\rangle$, $A_4^4\langle r_0^4\rangle$, $A_6^0\langle r_0^6\rangle$, and $A_6^4\langle r_0^6\rangle$. By Orbach's method, the parameters $A_2^m\langle r_0^2\rangle$ cannot be estimated. For the calculation in the last section, the $n=2$ terms are about $(R^2/\langle r_0^2\rangle)$

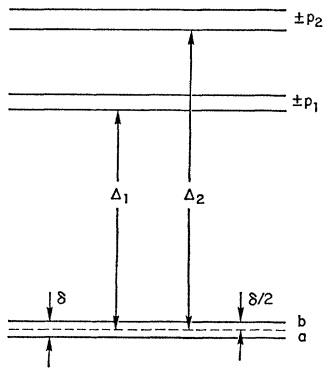

FIG. 1. A representative spin system of a Kramers salt.

stronger than the $n=4$ terms in most cases (for example, T_m^{2+} in CaF_2). Hence one can conclude that Orbach's theory is easier to use for crystals of lower symmetries for which the normal coordinates are harder to find, and for crystal of cubic symmetry, one should use the proper Van Vleck's theory.

4. Formulas of the Spin-Lattice Relaxation Times T_1

We shall restrict our case to the Kramers salts of the XY_8 symmetry only. Hence only the case shown in Fig. 1 will be discussed. Moreover, we are interested in the lattice temperature region in which Δ_1, $\Delta_2,\cdots\gg kT\gg\delta$. For convenience we shall define

$$a_{ji}\equiv A_j k_i = A_j(\omega_i/v)\,, \tag{23}$$

where A_j can be easily found from Eqs. (6) and (7) and v is the sound velocity. Therefore, if we follow Orbach's formalism[5] and use Van Vleck's interaction, Eq. (9), we get:

A. Direct Process

$$\frac{1}{T_1}=\frac{4H^4kTg^2\beta^2}{\pi\rho\hbar^4}\sum_{m=1}^{3}\frac{1}{v_m{}^5}\times\left|\sum_j\sum_{p_t}\frac{\langle\pm p_t|\mu_z|b\rangle\langle a|v_j|\pm p_t\rangle}{\Delta_i}\right|_{\rm av}^2, \tag{24}$$

where H is the dc magnetic field strength, g is the g factor, v_m is the sound velocity of the mth mode, μ_z is the z component of the magnetic moment operator, "av" means the average, and ρ is the density of the crystal.

B. Raman Process

In a temperature range $T\leq 0.1\Theta_D$, where Θ_D is the Debye temperature, the relaxation rate for a Raman process in a Kramers salt is given by

$$\frac{1}{T_1}=\sum_{\substack{m\\m'}=1}^{3}\frac{8!\hbar^2}{\pi^3\rho^2v_m{}^5v_{m'}{}^5}\left(\frac{kT}{\hbar}\right)^9\times\left|\sum_{j,k}\sum_{p_t}A_jA_k'\frac{\langle a|v_j|+p_t\rangle\langle+p_t|v_k'|b\rangle}{\Delta_{p_t}{}^2}\right|_{\rm av}^2. \tag{25}$$

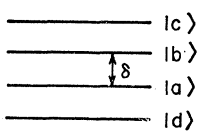

FIG. 2. Crystal field splitting of an S-state ion.

C. Orbach Process

$$\frac{1}{T_1}=\sum_{m=1}^{3}\sum_{p_t}\frac{1}{2\pi\rho v_m{}^5\hbar}\left(\frac{\Delta_{p_t}}{\hbar}\right)^3\left[\left|\sum_j A_j\langle a|v_j|+p_t\rangle\right|_{\rm av}{}^2+\left|\sum_j A_j\langle+p_t|v_j|b\rangle\right|_{\rm av}{}^2\right]^{-1}\left|\sum_{j,k}A_jA_k'\langle a|v_j|+p_t\rangle\times\langle+p_t|v_k'|b\rangle\right|_{\rm av}{}^2\exp(-\Delta_{p_t}/kT). \tag{26}$$

D. S-State Ions

For the case of S-state ions, the crystalline field splittings are so small that any spin-orbit state can be equivalently considered as a multilevel state. For simplicity a system as shown in Fig. 2 will be considered. In order to find T_1 for this multilevel system, we have to solve the rate equations. However, approximately, the relaxation rate between $|a\rangle$ and $|b\rangle$ in the temperature region δ, Δ_1, $\Delta_2,\cdots\ll\hbar\omega\sim kT$, is given by

$$\frac{1}{T_1}=\sum_{\substack{m\\m'}=1}^{3}\frac{8\cdot4!}{\pi^3\rho^2v_m{}^5v_{m'}{}^5\hbar^2}\left(\frac{kT}{\hbar}\right)^5\times\sum_{j,k}\sum_i A_jA_k'\langle a|v_j|i\rangle\langle i|v_k'|b\rangle|_{\rm av}{}^2, \tag{27}$$

a relation which was first predicted by Orbach and Blume[9] for Sm^{3+} in a field of cubic symmetry.

III. RESULTS

The pulsed saturation method[10] at 8.9 kMc/sec, very similar to that used by Scott and Jeffries,[11] was used to measure the spin-lattice relaxation time. The temperature was measured from the vapor pressure of liquid helium and liquid hydrogen and from the resistance of a 50-Ω carbon resistor.

The Ho^{2+}- and the Tm^{2+}-doped CaF_2 crystals were supplied by Sabisky of RCA and the Eu^{2+}-doped CaF_2 samples by Shen of Harvard University. The Yb^{3+}- and the Nd^{3+}-doped diamagnetic garnets were grown by Wolf of Yale University, Rimai of Raytheon Company and Molea of Harvard University. The Sm^{3+}-in-LES samples were supplied by Seidel of Brown University.

[9] R. Orbach and M. Blume, Phys. Rev. Letters **8**, 478 (1962).
[10] C. F. Davis, Jr., M. W. P. Strandberg, and R. L. Kyhl, Phys. Rev. **111**, 1268 (1958).
[11] P. L. Scott and C. D. Jeffries, Phys. Rev. **127**, 32 (1962).

1. Tm^{2+} in CaF_2

Paramagnetic resonance of Tm^{2+} in CaF_2 was first observed by Hays and Twidell[12] by x irradiating Tm^{3+} in CaF_2 samples at 77°K. Their data show that $g=3.453$ and $A=228$ G. The optical spectrum of Tm^{2+} in CaF_2 has been observed by Kiss.[13] He found that the Γ_7 doublet lies lowest ($E=0$) in agreement with Hays and Twidell's data, with a quartet Γ_8 at 555.8 cm^{-1}. The position of the Γ_6 doublet could not be located experimentally because the lines to identify it come on the steep shoulders of the strong vibrational line and cannot be seen. According to Bleaney's point-charge calculations,[14] this level is at 588 cm^{-1} above the ground doublet Γ_7 (see Fig. 3).

Figure 4 shows the results for T_1^{-1} at $H=1.92$ and 2.15 kG for the two hyperfine components of a 0.2% Tm^{2+} in CaF_2 crystal along the crystal orientation [100]. The data in the temperature range $1.25\leq T\leq 22$°K are very well fitted by the expression

$$1/T_1=13T+7.7\times10^{-8}T^9 \text{ sec}^{-1}, \quad (28)$$

which can be interpreted as representing the true relaxation rate for a direct process plus a Raman process for a Kramers salt. The linewidth at 77°K is broader than that at 4.2°K (12 G) by 43 G corresponding to $T_1\simeq1.6\times10^{-8}$ sec, which is about 20 times longer than the value, 0.9×10^{-9} sec, obtained from Eq. (28). This is as expected because the low-temperature approximation of the transport integral, J_8, is no longer valid at liquid-nitrogen temperature ($77°K>0.1\Theta_D\simeq50°K$).

The zeroth-order electronic wave functions for $J=\frac{7}{2}$ in a cubic field are[15]

$$\begin{aligned}
\Gamma_7:\quad & |a\rangle=\tfrac{1}{2}[(3)^{1/2}|-\tfrac{5}{2}\rangle-|+\tfrac{3}{2}\rangle],\\
& |b\rangle=\tfrac{1}{2}[(3)^{1/2}|+\tfrac{5}{2}\rangle-|-\tfrac{3}{2}\rangle],\\
\Gamma_8:\quad & |p_{11}\rangle=(7/12)^{1/2}[|+\tfrac{7}{2}\rangle-5/(35)^{1/2}|-\tfrac{1}{2}\rangle],\\
& |p_{12}\rangle=(7/12)^{1/2}[|-\tfrac{7}{2}\rangle-5/(35)^{1/2}|+\tfrac{1}{2}\rangle],\\
& |p_{13}\rangle=\tfrac{1}{2}[|+\tfrac{5}{2}\rangle+(3)^{1/2}|-\tfrac{3}{2}\rangle],\\
& |p_{14}\rangle=\tfrac{1}{2}[|-\tfrac{5}{2}\rangle+(3)^{1/2}|+\tfrac{3}{2}\rangle],\\
\Gamma_6:\quad & |p_{21}\rangle=(5/12)^{1/2}[|+\tfrac{7}{2}\rangle+7/(35)^{1/2}|-\tfrac{1}{2}\rangle],\\
& |p_{22}\rangle=(5/12)^{1/2}[|-\tfrac{7}{2}\rangle+7/(35)^{1/2}|+\tfrac{1}{2}\rangle].
\end{aligned} \quad (29)$$

For our calculations the mean radii calculated by Freeman and Watson[16] will be used. They are tabulated in Table I.

TABLE I. Mean radii of Tm^{2+}, Eu^{2+}, Ho^{2+}, Yb^{3+}.

	Tm^{2+}	Eu^{2+}	Ho^{2+}	Yb^{3+}
$\langle r_0^2\rangle$	0.728	0.938	0.763	0.613
$\langle r_0^4\rangle$	1.552	2.273	1.515	0.960
$\langle r_0^6\rangle$	7.510	11.67	7.78	3.104

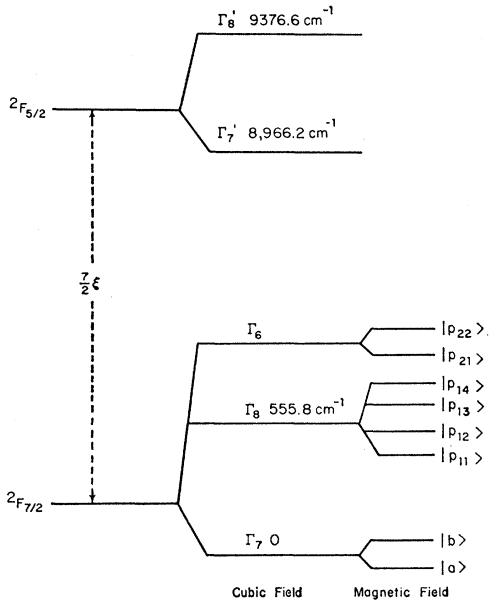

FIG. 3. Splitting of the $F_{7/2}$ state of Tm^{2+} in the calcium fluoride crystal field and the magnetic field.

In order to calculate the relaxation rate from Eqs. (24) and (25), the following average values, making use of the average values of the direction cosines calculated by Van Vleck,[4] are needed:

$$(\langle A_j^2\rangle_{\text{av}})_{\text{longitudinal}}=(32\pi^2R^2/15)=3.93\times10^{-15}\text{ cm}^2, \quad (30)$$

$$(\langle A_j^2\rangle_{\text{av}})_{\text{transverse}}=(8\pi^2R^2/5)=2.93\times10^{-15}\text{ cm}^2, \quad (31)$$

$$(j=2,3,4,5,6)$$

in which $R=2.726$ Å is used.

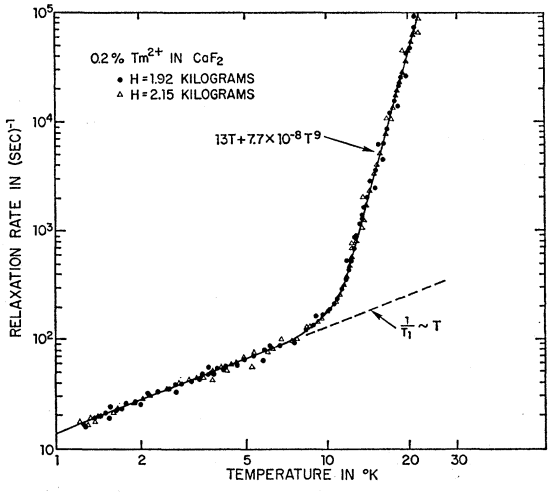

FIG. 4. Relaxation data for 0.2% Tm^{2+} in CaF_2. The data are fit better by $1/T_1=13T+1.1\times10^{-8}T^9$ sec^{-1}.

[12] W. Hays and J. W. Twidell, J. Chem. Phys. **35**, 1521 (1961).
[13] Z. J. Kiss, Phys. Rev. **127**, 718 (1962).
[14] B. Bleaney, Proc. Roy. Soc. (London) **A277**, 289 (1964).
[15] C. Kittel and J. M. Luttinger, Phys. Rev. **73**, 162 (1948).
[16] A. J. Freeman and R. E. Watson (to be published).

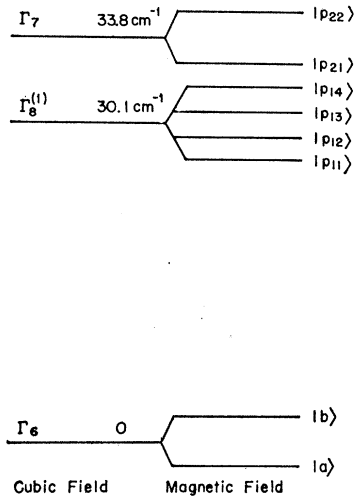

FIG. 5. Splitting of the lowest state of Ho^{2+} in the CaF_2 crystal field and the magnetic field (not to scale).

With the aid of the reduced matrix elements calculated by Prather[17] and the Clebsch-Gordan coefficients tabulated by Rotenberg *et al.*,[18] one predicts

$$1/T_1=4.5T+1.9\times10^{-6}T^9 \text{ sec}^{-1} \tag{32}$$

in which $\rho=3.21$ g/cm^3, $v_l=7.36\times10^5$ cm/sec and $v_t=3.34\times10^5$ cm/sec are used. On comparison of Eq. (32) with Eq. (28), the calculation of the direct process is seen to be in quite good agreement with the measurements, but that of the Raman process gives a relaxation rate greater by a factor 20 than the measured relaxation rate. However, considering the many approximations in the theory, the estimated relaxation rate given by Eq. (32) is quite acceptable.

It is interesting to see that our dynamic crystalline field is about 15 times greater than that obtained from the cubic field parameters based on Eq. (19). This fact shows that Orbach's theory will give the relaxation time in a direct-process region $\sim$200 times longer than ours.

2. Ho^{2+} in CaF_2

The ground state of the free Ho^{2+} ion is $^4I_{15/2}$. In a cubic field, this 16-fold degeneracy will be split into two doublets Γ_6 and Γ_7 and three quartets $\Gamma_8^{(1)}$, $\Gamma_8^{(2)}$, and $\Gamma_8^{(3)}$. The optical spectrum first observed by Weakliem and Kiss[19] shows that there are a quartet $\Gamma_8^{(1)}$ at 30.1 cm^{-1} and a doublet Γ_7 at 33.8 cm^{-1} above the ground-state doublet Γ_6 (Fig. 5). With these data and the aid of the theoretical calculations by Lea *et al.*,[20] one finds that $\Gamma_8^{(2)}$ and $\Gamma_8^{(3)}$ are well separated from the ground-state doublet Γ_6 by 480 cm^{-1}, approximately, and, therefore, are not important in the relaxation calculation. The paramagnetic resonance spectrum has been observed by Sabisky and Lewis.[21] They give $g=5.911$ and $A=0.1308$ cm^{-1}.

The relaxation-time measurements have been made for the $|J_z=+\frac{1}{2}, I_z=-\frac{7}{2}\rangle\rightarrow|J_z=-\frac{1}{2}, I_z=-\frac{7}{2}\rangle$ transition at 2.4 kG of a 0.02% Ho^{2+} in CaF_2 crystal along [100]. The data are given in Fig. 6 and are well fitted by the expression

$$1/T_1=42T+8.0\times10^9\exp(-33.1\times1.44/T) \text{ sec}^{-1}, \tag{33}$$

clearly showing a direct process which is dominant for temperatures below 2°K and an Orbach process. The linewidths at liquid-hydrogen temperatures have been measured and the results agree very well with the last equation within experimental error as demonstrated in Fig. 6.

The wave functions can be also obtained from Lea *et al.*'s work[20]

$$\begin{aligned}
\Gamma_6:&\left\{\begin{matrix}|a\rangle\\|b\rangle\end{matrix}\right\}=0.5818|\pm\tfrac{5}{2}\rangle-0.3307|\pm\tfrac{7}{2}\rangle\\
&\qquad-0.7182|\mp\tfrac{1}{2}\rangle+0.1910|\mp\tfrac{9}{2}\rangle\\
\Gamma_7:&\left\{\begin{matrix}|p_{21}\rangle\\|p_{22}\rangle\end{matrix}\right\}=0.6332|\pm13/2\rangle+0.5819|\pm\tfrac{5}{2}\rangle\\
&\qquad-0.4507|\mp\tfrac{3}{2}\rangle-0.2393|\mp11/2\rangle\\
\Gamma_8^{(1)}:&\left\{\begin{matrix}|p_{11}\rangle\\|p_{12}\rangle\end{matrix}\right\}=0.7452|\pm15/2\rangle+0.1486|\pm\tfrac{7}{2}\rangle\\
&\qquad-0.6231|\mp\tfrac{1}{2}\rangle-0.18521|\mp\tfrac{9}{2}\rangle\\
&\left\{\begin{matrix}|p_{13}\rangle\\|p_{14}\rangle\end{matrix}\right\}=0.3149|\pm13/2\rangle-0.4074|\pm\tfrac{5}{2}\rangle\\
&\qquad+0.7851|\pm\tfrac{3}{2}\rangle+0.3442|\mp11/2\rangle.
\end{aligned} \tag{34}$$

No computation has been made for the mean radii of the divalent holmium ion. With the calculated mean radii of Eu^{2+} we can extrapolate them by using the Elliott and Stevens formula[22]

$$\langle r_0^n\rangle\propto(Z-55)^{-n/4}. \tag{35}$$

We now calculate the relaxation rate from Eqs. (24), (25), and (26). We find

$$\begin{aligned}
1/T_1=37T&+8.5\times10^9\exp(-33.8\times1.44/T)\\
&+8.5\times10^7\exp(-30.1\times1.44/T)\\
&+2.1\times10^{-4}T^9 \text{ sec}^{-1}.
\end{aligned} \tag{36}$$

The third term of the last equation is about two orders of magnitude and the last term is about four orders of magnitude smaller than the second term in the temperature range we are interested, so that these two terms are negligible. By comparing Eq. (36) with Eq. (33),

[17] J. L. Prather, National Bureau of Standards Monograph 19, 1961.
[18] M. Rotenberg, R. Bivins, N. Metropolis, and J. K. Wooten, Jr., *The 3-j and 6-j Symbols* (The Technology Press, Massachusetts Institute of Technology, Cambridge, Massachusetts, 1959).
[19] H. Weakliem and Z. J. Kiss (to be published).
[20] K. R. Lea, M. J. M. Leask, and W. P. Wolf, J. Phys. Chem. Solids **23**, 1381 (1962).
[21] E. S. Sabisky and H. R. Lewis, Proc. IEEE **51**, 53 (1963); Phys. Rev. **130**, 1370 (1963).
[22] R. J. Elliott and K. W. H. Stevens, Proc. Roy. Soc. (London) **A215**, 437 (1952).

TABLE II. g values of Yb^{3+} in YGaG, YAlG, LGaG, and Nd^{3+} in YGaG, YAlG.

	Yb^{3+}			Nd^{3+}	
	YGaG	YAlG	LGaG	YGaG	YAlG
g_x	3.73	3.87	3.65	2.03	1.733
g_y	3.60	3.78	3.56	1.25	1.179
g_z	2.85	2.47	2.99	3.67	3.92

we find that our theoretical calculation agrees extremely well with the experimental data.

3. Yb^{3+} in Yttrium Gallium Garnet (YGaG)

The free ion of Yb^{3+} is isoelectronic to Tm^{2+}. It is known from the x-ray and the neutron diffraction data[6] that the oxygen ions coordinated to the rare-earth ions in the garnets are located at the vertices of a distorted cube. The point symmetry at the rare-earth site is D_2.

Paramagnetic resonance spectra of rare-earth ions in diamagnetic garnets have been reported by Wolf and co-workers at Oxford[23] and by Carson *et al.*[24] The g values are tabulated in Table II. Energy levels associated with the crystalline field splitting have been

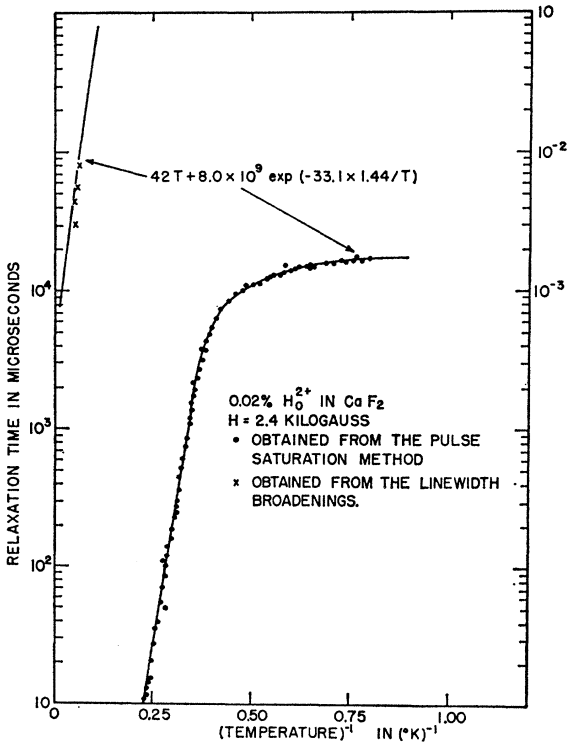

FIG. 6. Relaxation data for 0.02% Ho^{2+} in CaF_2. The data are better fitted by $1/T_1=42T+8.0\times10^9\exp(33.1\times1.44/T)$ sec^{-1}.

[23] W. P. Wolf, M. Ball, M. T. Hutchings, M. J. M. Leask, and A. F. G. Wyatt, J. Phys. Soc. Japan **17**, Suppl. B-I, 443 (1962).
[24] J. W. Carson and R. L. White, J. Appl. Phys. **31**, 535 (1960).

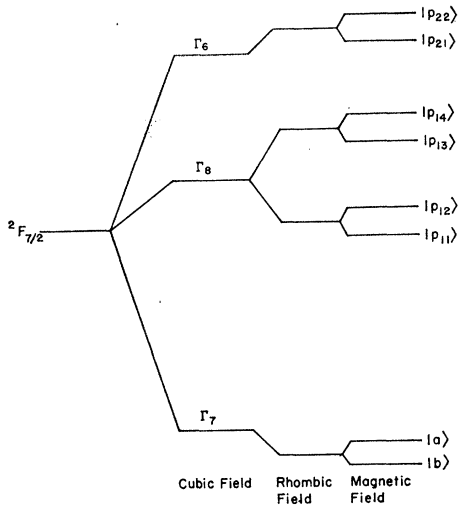

FIG. 7. Splitting of the lowest state of Yb^{3+} in a rhombic field and a magnetic field (not to scale).

essayed by many groups. Ball,[25] Ayant,[26] Brumage,[27] and Hutchings[28] have reported that the quartet is about 550 cm^{-1} above the ground doublet Γ_7. However, from the data of the temperature dependence of the intensity of the optical transition, Wood[29] has claimed that there are electronic levels at 112 and 308 cm^{-1}. For our purpose, we shall take $E(\Gamma_6)-E(\Gamma_7)$ to be 800 cm^{-1}, $E(\Gamma_8)-E(\Gamma_7)$ to be 550 cm^{-1}, and consider the 112 cm^{-1} level as a vibrational state of the lattice as suggested by Tinkham.[30]

The measurements of the spin-lattice relaxation time were made at $H=1.75$ kG along [100] where two lines meet and the resonance is well separated from another resonance in order to reduce the effect of cross relaxation. The data for 0.1% Yb^{3+} in YGaG below 20°K are plotted in Fig. 8 and can be fitted by the expression

$$1/T_1=33T+1.8\times10^{-7}T^9 \text{ sec}^{-1}. \quad (37)$$

This temperature dependence indicates that the relaxation consists of a direct process plus a Raman process for a Kramers salt at low temperatures when the energy splitting to the first excited state is larger than the Debye energy. In consequence of this fact the 112 cm^{-1} level should be a vibrational state of the lattice.

The measurements of the 1% sample agree very well with those of the 0.1% sample in the Raman region but deviate at low temperatures. Below 10°K the measured

[25] M. Ball, G. Garton, M. J. M. Leask, and W. P. Wolf, *Proceedings of the Seventh International Conference on Low-Temperature Physics, 1960* (University of Toronto Press, Toronto, 1960), p. 128.
[26] Y. Ayant and J. Thomas, Compt. Rend. **248**, 387 (1959).
[27] W. H. Brumage, C. C. Lin, and J. H. Van Vleck, Phys. Rev. **132**, 608 (1963).
[28] M. T. Hutchings and W. P. Wolf (to be published).
[29] D. L. Wood, J. Chem. Phys. **39**, 1671 (1963).
[30] A. J. Sievers, III, and M. Tinkham, Phys. Rev. **129**, 1995 (1963).

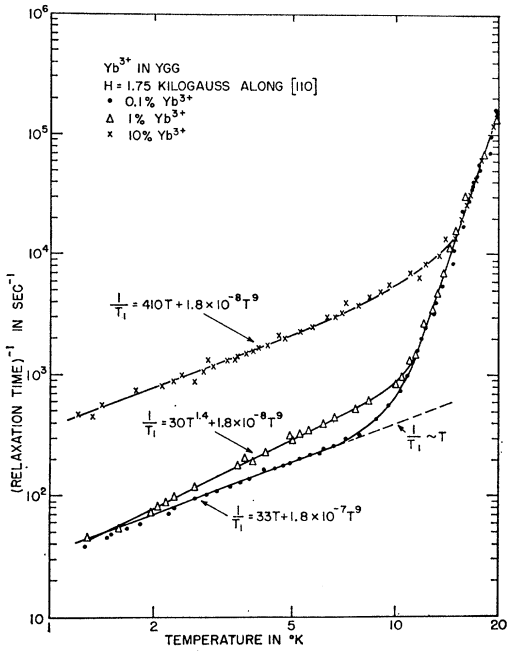

FIG. 8. Relaxation data for 0.1, 1, and 10% Yb^{3+} in YGaG.

data can be described by

$$1/T_1=30T^{1.4}\ \text{sec}^{-1}. \tag{38}$$

This temperature dependence could be interpreted as arising from an additional contribution to the relaxation rate from exchange coupled pairs.[31] This interpretation is supported by the data of the 10% Yb sample which are well fitted by

$$1/T_1=410T\ \text{sec}^{-1} \tag{39}$$

at low temperatures because the contribution to the relaxation due to the exchange interaction[32] for this highly concentrated sample is presumably dominant.

For our calculation the cubic wave functions for $J=\frac{7}{2}$ given in Eq. (29) will be used because of the facts that the excited states are rather elevated and the orbit-lattice interaction is insensitive to a small distortion. Taking $e'=2e$ and $2R=2.77$ Å, $\rho=5.17$ g/cm^3, $v_t=3.84\times10^5$ cm/sec, $v_l=7.153\times10^5$ cm/sec, one finds

$$1/T_1=4.2T+5.7\times10^{-7}T^9\ \text{sec}^{-1}. \tag{40}$$

The last equation shows that our theoretical estimate is in good agreement with the experimental data, Eq. (37).

[31] *Advances in Quantum Electronics*, edited by J. R. Singer (Columbia University Press, New York, 1962); N. Bloembergen and P. S. Pershan, *ibid.* p. 377; J. H. Van Vleck, *ibid.* p. 388; J. C. Gill and R. J. Elliott, *ibid.* p. 399.

[32] R. Orbach, *Proceedings of the First International Conference on Paramagnetic Resonance* (Academic Press Inc., New York, 1963), Vol. II, p. 456.

4. Yb^{3+} in Yttrium Aluminum Garnet (YAlG)

From a complex fluorescence spectrum Wood[29] has reported that there are levels at 0, 140, 490, and 620 cm^{-1} for Yb^{3+} in YAlG. Again, we shall exclude the 140-cm^{-1} level as a vibrational state of the lattice.

The measurements were made for a 0.1% and a 1% samples at $H=1.77$ kG applied along [100]. The measured data for the 0.1% sample are shown in Fig. 9 and fit the equation

$$1/T_1=15T+6.3\times10^{-7}T^9\ \text{sec}^{-1}. \tag{41}$$

The last equation clearly displays a direct and a Raman process. The results for the 1% sample yield a best fit described by

$$1/T_1=11T^{2.3}+6.3\times10^{-7}T^9\ \text{sec}^{-1}. \tag{42}$$

The first term of the last equation looks like a phonon bottleneck. However, it is very unlikely to have a phonon bottleneck at $T=10$°K. Compared with the data for the 0.1% sample, we could interpret it as arising from the contribution to relaxation from exchange coupled pairs. Equations (41) and (42) are in reasonable agreement with Carson and White's data[24] at 4.2°K obtained from a cw method, but are too large compared with the results obtained from the pulsed-field EPR spectra by Rimai *et al.*[33] who give at liquid-helium temperatures,

$$1/T_1\simeq1.7\times10^{-2}T\ \text{sec}^{-1} \tag{43}$$

extrapolated to 9 kMc/sec.

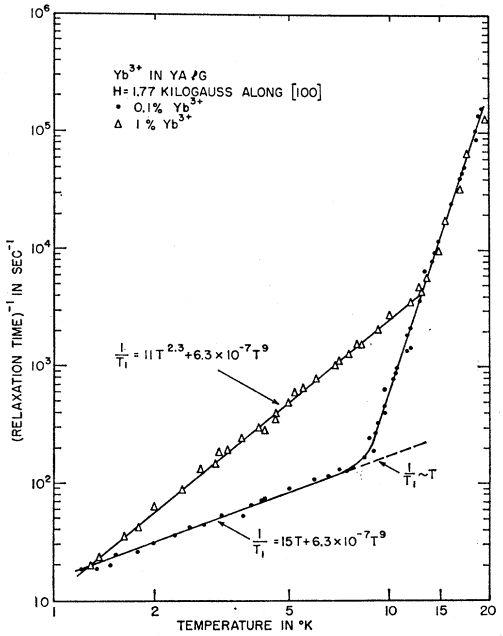

FIG. 9. Relaxation data for 0.1 and 1% Yb^{3+} in YAlG.

[33] L. Rimai, B. D. Silverman, and R. W. Bierig, Bull. Am. Phys. Soc. **9**, 37 (1964).

With the data given above and given in the last section, Eqs. (24) and (25) yield an estimated relaxation rate

$$1/T_1=5.3T+9.0\times10^{-7}T^9 \text{ sec}^{-1} \quad (44)$$

which is in a quite good agreement with the measurements for the one-phonon direct and the two-phonon Raman processes given by Eq. (42).

5. Yb^{3+} in Lutetium Gallium Garnet (LGaG)

The relaxation data were taken for a 1% sample at $H=1.43$ kG along [100] and are well fitted by the equation

$$1/T_1=9.8T^{1.7}+1.0\times10^{-7}T^9 \text{ sec}^{-1}, \quad (45)$$

as shown in Fig. 10. The first term is again interpreted as arising from exchange coupled pairs, and the last term suggests the first excited state to be roughly around 650 cm^{-1}. Based on the experience we have had for the cases for Yb^{3+} in YGaG and YAlG, we might assume the relaxation time of the isolated spins to be the same with that of the 1% sample at $T=1.3°K$ (see Fig. 10) so that the relaxation rate is

$$1/T_1=12T+1.0\times10^{-7}T^9 \text{ sec}^{-1}. \quad (46)$$

This is in good agreement with the theoretical calculation which predicts

$$1/T_1\approx3.1T+3.2\times10^{-7}T^9 \text{ sec}^{-1}. \quad (47)$$

6. Nd^{3+} in Yttrium Gallium Garnet (YGaG)

The ground state of the free neodymium ion is $^4I_{9/2}$. In a cubic field this tenfold degeneracy splits into a doublet Γ_6 and two quartets $\Gamma_8^{(1)}$ and $\Gamma_8^{(2)}$. Kiss[34] from his studies of the optical absorption and fluorescence spectra of Nd^{3+} in cubic sites of CaF_2 has reported that the $\Gamma_8^{(1)}$ quartet and the Γ_6 doublet are, respectively, 180 and 700 cm^{-1} above the ground quartet $\Gamma_8^{(2)}$ and the first excited multiplet is about 2000 cm^{-1} above $\Gamma_8^{(2)}$. In a rhombic field, $\Gamma_8^{(2)}$ further splits into two doublets as shown in Fig. 11. In consequence of the fact that the first excited state is low, the cubic approximation is no longer a good approximation, and, therefore, the theoretical prediction of T_1 based on the cubic approximation is not feasible.

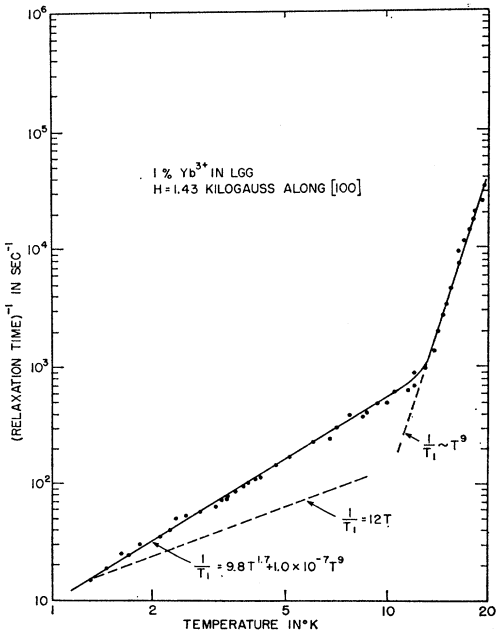

FIG. 10. Relaxation data 1% Yb^{3+} in LGG.

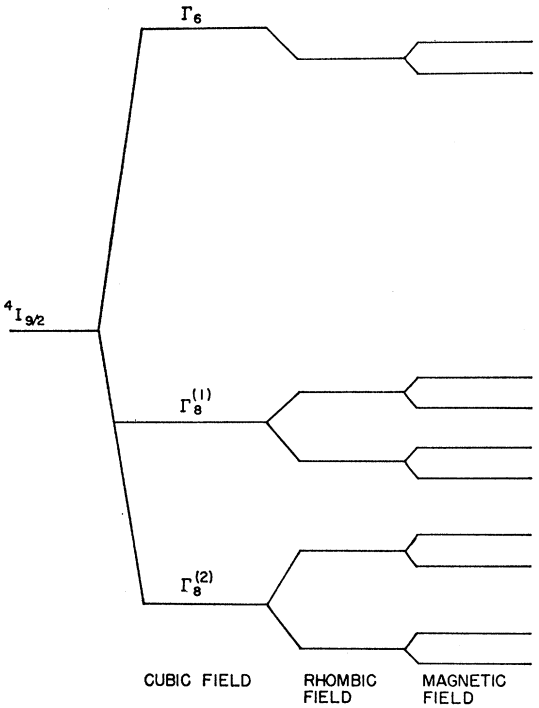

FIG. 11. Splitting of the lowest state of Nd^{3+} in YGaG (not to scale).

The measurements were made for two 1% samples at $H=2.32$ kG applied along [110], where the absorption is strongest. The smooth curve drawn through the experimental points shown in Fig. 12 is expressed by

$$1/T_1=17T+9.0\times10^{10}\exp(-85\times1.44/T) \text{ sec}^{-1}, \quad (48)$$

which clearly shows a direct and an Orbach process with an excited state 85 cm^{-1} above the ground doublet.

7. Nd^{3+} in Yttrium Aluminum Garnet (YAlG)

The relaxation times of a 1% Nd^{3+} in YAlG crystal were measured at $H=1.9$ kG along the [110] orientation of the crystal. The experimental data, as shown in Fig. 13, appear to fit reasonably well to the sum of a term linear in T and an exponential term,

$$1/T_1=34T+4.5\times10^{10}\exp(-75\times1.44/T) \text{ sec}^{-1}. \quad (49)$$

[34] Z. J. Kiss, J. Chem. Phys. 38, 1476 (1963).

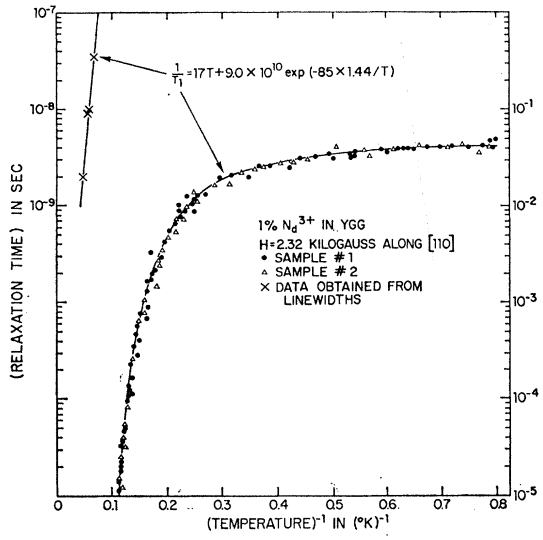

FIG. 12. Relaxation data for 1% Nd^{3+} in YGaG.

So far, no optical determination[35] of the crystalline field splitting is available for comparison.

8. Sm^{3+} in LES

The ground and the first excited multiplets[36] are, respectively $^6H_{5/2}$ and $^6H_{7/2}$, where the latter is about 1100 cm^{-1} above the former. In a crystalline field with a C_{3h} symmetry, the ground multiplet is split into three doublets, as shown in Fig. 14. Lammerman[37] from her optical measurements has reported the lowest state of this ground multiplet to be a doublet characterized by $|\frac{5}{2},\pm\frac{1}{2}\rangle$ with a $|\frac{5}{2},\pm\frac{3}{2}\rangle$ level at 53.8 cm^{-1} and a $|\frac{5}{2},\pm\frac{5}{2}\rangle$ level at 63.6 cm^{-1}.

Using the improved Orbach phenomenological orbit-lattice interaction,

$$(V_{01})_0'=\sum_{n,m} p_n V_n{}^m \epsilon_{nm}=\sum_{n,m} p_n A_n{}^m\langle r_0{}^n\rangle Y_n{}^m \epsilon_{nm} \quad (50)$$

one easily finds[5,36]

$$\frac{1}{T_1}=\sum_{p_t}\frac{2(g\beta H)^2}{\pi\rho v^5\hbar^4\Delta_{p_t}{}^2}|\mathbf{H}\cdot\langle -p_t|\mathbf{L}+2\mathbf{S}|b\rangle \times\langle a|\sum_{n,m} p_n V_n{}^m|-p_t\rangle|^2+\sum_{p_t}\frac{9!\hbar^2}{\pi^3\rho^2 v^{10}\Delta_{p_t}{}^4}\left(\frac{kT}{\hbar}\right)^9 \times|\sum_{\substack{n,m\\ n'm'}}\langle a|p_n V_n{}^m|-p_t\rangle\langle -p_t|p_{n'}V_{n'}{}^{m'}|b\rangle|^2, \quad (51)$$

where

$$g_{\parallel}{}^2=g^2\cos^2\Theta+g_{\perp}{}^2\sin^2\Theta,$$

Θ being the angle H makes with the symmetry axis of the crystal. Based on the last equation and the wave-functions. Orbach[36] was able to predict anisotropy in T_1 in the temperature region where direct processes predominate.

The paramagnetic resonance has been reported by Bogle and Scovil.[38] They gave $g_{\parallel}=0.596$ and $g_{\perp}=0.604$. The over-all temperature dependence of the relaxation

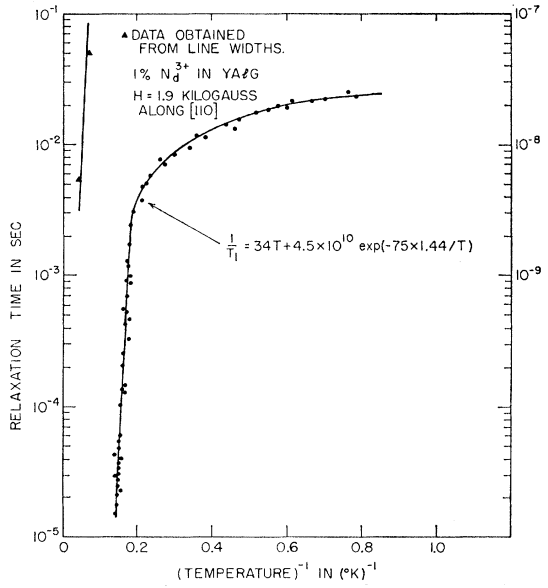

FIG. 13. Relaxation data for 1% Nd^{3+} in YAlG.

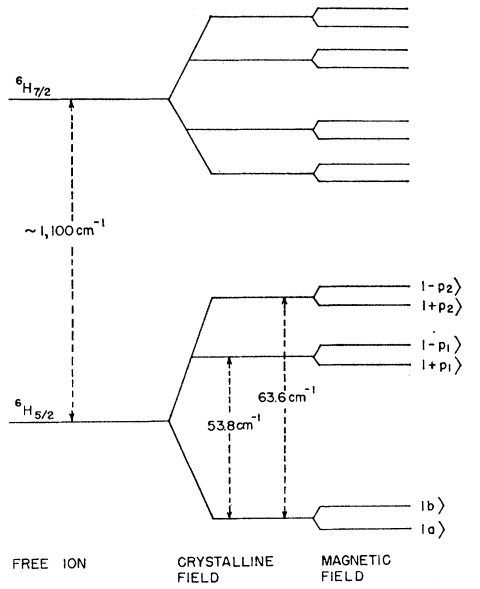

FIG. 14. A schematic energy-level diagram for Sm^{3+} in ethyl sulphate (not to scale).

[35] After the completion of this manuscript, Koningstein and Geusic [Phys. Rev. **136**, A711 (1964)] have reported $\Delta=135$ cm^{-1}. In this case, the second term of Eq. (49) might be brought about by the spin-optical phonon relaxation [C. Y. Huang, doctoral thesis, Harvard University, 1964 (unpublished)].

[36] R. Orbach, Phys. Rev. **126**, 1349 (1962).

[37] H. Lammerman, Z. Physik **150**, 551 (1958).

[38] G. S. Bogle and H. E. D. Scovil, Proc. Phys. Soc. (London) **A65**, 368 (1952).

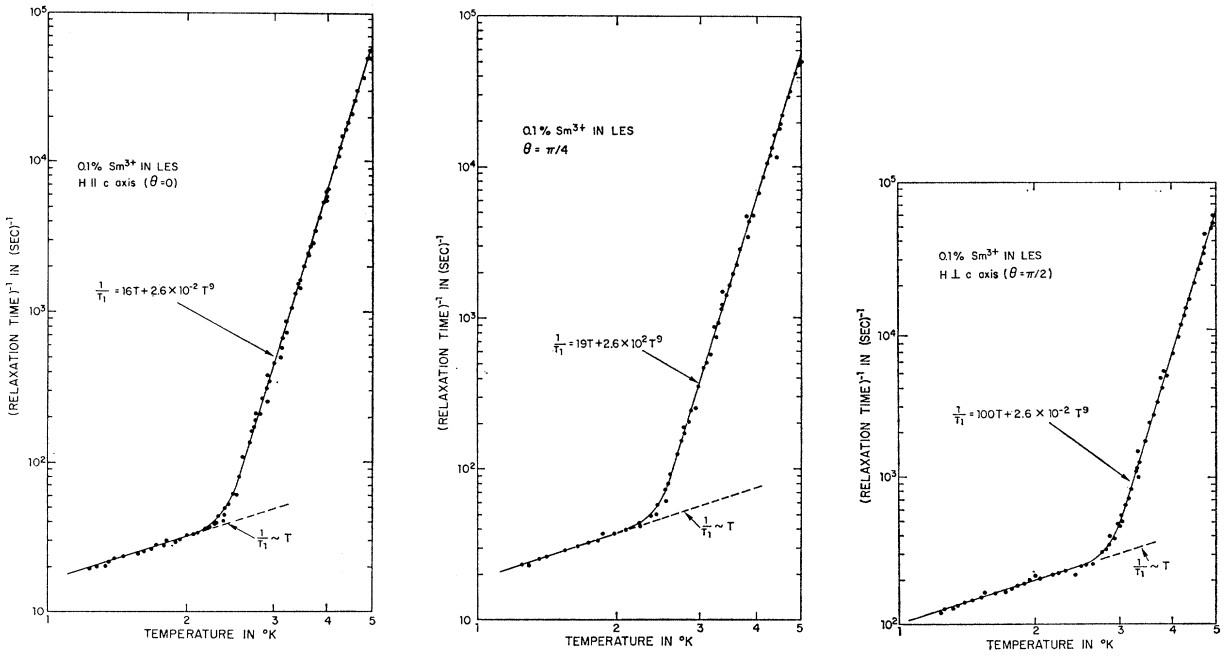

(a) (b) (c)

FIG. 15. (a) Relaxation data for 0.1% Sm^{3+} in LES, $H_{\parallel}$ c axis. (b) Relaxation data for 0.1% Sm^{3+} in LES, $\theta=\pi/4$. (c) Relaxation data for 0.1% Sm^{3+} in LES, $H_{\perp}$ c axis.

data for two 0.1% samples, as illustrated in Figs. 15(a), (b), and (c), can be fitted by

$$1/T_1=16T+2.6\times10^{-2}T^9\ \text{sec}^{-1}, \quad (52a)$$

$$=19T+2.6\times10^{-2}T^9\ \text{sec}^{-1}, \quad (52b)$$

$$=100T+2.6\times10^{-2}T^9\ \text{sec}^{-1}, \quad (52c)$$

for $\Theta=0$, $\pi/4$, and $\pi/2$, respectively, As shown in Fig. 16, the angular variation of the relaxation time was measured at the lowest attainable temperature 1.24°K in the cryogenic system used. The relaxation time varies by a factor of about 6 in rotating the magnetic field from a direction parallel to the c axis to the perpendicular direction.

Because Δ_{p_1} and Δ_{p_2} are too large to allow an Orbach process, with the aid of the normalized wave functions calculated by Orbach[36] and the crystal field parameters found by Powell and Orbach,[39] one finds

$$1/T_1=0.32T+4.4\times10^{-3}T^9\ \text{sec}^{-1}, \quad (53a)$$

$$1/T_1=1.8T+4.4\times10^{-3}T^9\ \text{sec}^{-1}, \quad (53b)$$

for $\Theta=0$ and $\pi/2$, respectively. In the direct process region, the last equations indicate an anisotropy by a factor ~6 instead of ~400 in rotating the magnet from a direction perpendicular to a direction parallel to the c axis of the crystal because the matrix elements for a magnetic field applied parallel to the c axis are greater than those for a field in a perpendicular direction. Comparing Eqs. (52) with (53), we notice that our theoretical estimates do not agree with the measured data within an order of magnitude. Nevertheless, since our calculations depend so much on the magnitudes of the roughly estimated $A_n{}^m\langle r_0{}^n\rangle$, Eqs. (53) are quite acceptable. The agreement would be worse if the factors p_n in Eq. (51) were dropped.

[39] M. J. D. Powell and R. Orbach, Proc. Phys. Soc. (London) A78, 753 (1961).

9. Eu^{2+} in CaF_2

The divalent europium ion belongs to the configuration $(4f)^7$. Its ground state is, in first approximation, ${}^8S_{7/2}$. The action of a crystal field of cubic symmetry lifts partially this eightfold degeneracy decomposing the ground state into two doublets Γ_6 and Γ_7 and a

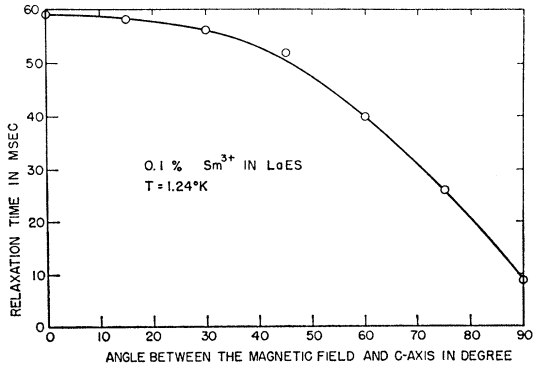

FIG. 16. Angular variation of the relaxation time.

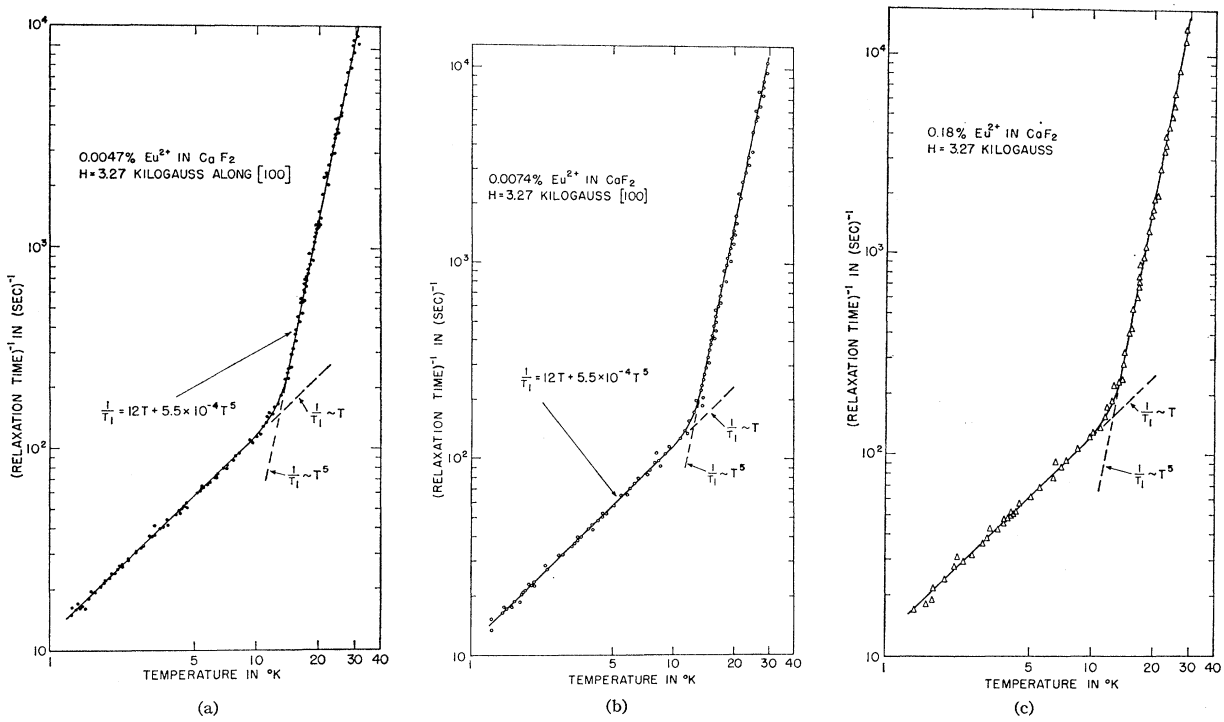

FIG. 17. (a) Relaxation data for 0.0047% Eu^{2+} in CaF_2. (b) Relaxation data for 0.0074% Eu^{2+} in CaF_2. (c) Relaxation data for 0.18% Eu^{2+} in CaF_2.

quartet, Γ_8. By means of paramagnetic resonance, Ryter[40] has found the total separation of the ground state to be 0.1784 cm^{-1} with $E(\Gamma_8)-E(\Gamma_7)=0.1107$ cm^{-1}, and $E(\Gamma_6)-E(\Gamma_7)=0.0677$ cm^{-1}. By the application of a static magnetic field, these Stark levels give rise to eight levels. Furthermore, each of these fine structure levels is accompanied by a hyperfine structure due to the coupling between electronic and nuclear moments.

The relaxation time measurements were made for the 0.0047, 0.0074, and 0.18% crystals. On saturating by pulses of duration ~ 50 μsec, it was noticed that the relaxation curve of the recovery of the absorption line intensity after the action of the saturation pulses at 4.2°K can be described by two characteristic times. When very short pulses of duration ~ 2.5 μsec were applied, the relaxation curve could be characterized by a short relaxation time depending on which hyperfine component the pulses were applied to. The fact that these short relaxation times are independent of temperature indicates that these relaxation times are in fact characteristic of the spin-spin interaction and are identified as spin-spin cross-relaxation times, T_{12}. This cross relaxation may be brought about by the transition between different components of the hyperfine structure corresponding to the same electronic transition. Because there are two odd isotopes, Eu^{151}, and Eu^{153}, it is very difficult to give a definite interpretation of the observed cross relaxation since there are so many routes by which cross-relaxation processes may proceed. In order to eliminate this cross-relaxation effect, broad pulses were used. During the time of action of the saturation pulse, the duration of which is greater than the cross-relaxation time, the saturation processes within the spin system have time to get established, and after the saturating pulse only the spin-lattice relaxation time should be observed. However, the pulse duration should be short compared with T_1 and short enough such that no cross saturation over the neighboring electronic transition lines occurs. It turned out that only one line, corresponding to the $+\frac{1}{2}\rightarrow-\frac{1}{2}$ electronic transition for a magnetic field applied along a fourfold axis, with pulses of duration $2\geq\tau\geq 0.5$ msec, showed the relaxation curve in the form of only one slowly falling exponential because only this line is well separated from the rest such that the cross relaxations among different electronic transitions within each component of the hyperfine structure was avoided. Thus the characteristic time corresponding to this exponential which depends on T^{-1} is the spin-lattice relaxation time T_1. Consequently, the recovery traces for the intermediate pulse duration consists of a mixture of the spin-lattice relaxation and the spin-spin cross-relaxation processes. The measured data as shown in Figs. 17(a), (b), and (c) for 0.0047, 0.0074, and 0.18% samples, respectively, are well fitted by the smooth curves described by

$$1/T_1=12T+5.3\times10^{-4}T^5 \text{ sec}^{-1}. \quad (54)$$

The independence of T_1 of concentration clearly indi-

[40] C. Ryter, Helv. Phys. Acta **30**, 395 (1957).

TABLE III. Comparison of measured data and theoretical estimates of the spin-lattice relaxation rates for rare-earth ions in single crystals.

Salt		Direct process T_1^{-1} in $(\text{sec})^{-1}$	Orbach process T_1^{-1} in $(\text{sec})^{-1}$	Raman process T_1^{-1} in $(\text{sec})^{-1}$
0.2% Tm^{2+} in CaF_2	meas	$13T$		$7.7\times10^{-8}T^9$
	theoret	$4.5T$		$1.9\times10^{-6}T^9$
0.02% Ho^{2+} in CaF_2	meas	$42T$	$8.0\times10^9\exp(48/T)$	
	theoret	$37T$	$8.5\times10^9\exp(48.7/T)$	
0.0047, 0.18, 0.0074T Eu^{2+} in CaF_2	meas	$12T$		$5.3\times10^{-4}T^5$
0.1% Yb^{3+} in YGaG	meas	$33T$		$1.8\times10^{-7}T^9$
	theoret	$4.2T$		$5.7\times10^{-7}T^9$
0.1% Yb^{3+} in YAlG	meas	$15T$		$6.3\times10^{-7}T^9$
	theoret	$5.3T$		$9.0\times10^{-7}T^9$
1% Nd^{3+} in YGaG	meas	$17T$	$9.0\times10^{10}\exp(-120/T)$	
	theoret	$10T$	$10^{12}\exp(-120/T)$	
1% Nd^{3+} in YAlG	meas	$34T$	$4.5\times10^{10}\exp(-110/T)$	
	theoret	$10T$	$10^{11}\exp(-110/T)$	
0.1% Sm^{3+} in LES	meas $H_{\|\|}$	$16T$		$2.6\times10^{-2}T^9$
	theoret $H_{\|\|}$	$0.32T$		$4.4\times10^{-3}T^9$
	meas $H_\perp$	$100T$		$2.6\times10^{-2}T^9$
	theoret $H_\perp$	$1.8T$		$4.4\times10^{-3}T^9$
	meas $H_{\pi/4}$	$19T$		$2.6\times10^{-2}T^9$
1% Yb^{3+} in YGaG	meas	$30T^{1.4}$		$1.8\times10^{-7}T^9$
10% Yb^{3+} in YGaG	meas	$410T$		$1.8\times10^{-7}T^9$
1% Yb^{3+} in LGaG	meas	$9.8^{1.7}$		$1.0\times10^{-7}T^9$
1% Yb^{3+} in YAlG	meas	$11T^{2.3}$		$6.3\times10^{-7}T^9$

cates that spin-spin cross-relaxation time mentioned above was brought about by the transition between different components of the hyperfine structure corresponding to the same electronic transition and that the long pulses do not cause cross relaxations with the neighboring lines. In consequence the measured characteristic times are the true spin-lattice relaxation times.

The theoretical estimation of the crystal field splittings for Gd^{3+} in CaF_2 has been attempted by Lacroix.[41–43] He has reported that the theory[42] based on only the admixtures of ^6P and ^6I predicts only one tenth of the experimental result and suggested[43] that the contribution from the relevant excited configurations, $(4f)^6(5f)$ and $(4f)^5(5d)^2$, is very important. Due to this fact the contribution to the relaxation by the odd vibrations could also be important. However, the estimation of T_1 in this unequally spaced multilevel system is not trivial and will not be discussed here.

Recently, Bierig *et al.*[44] reported that the spin-lattice relaxation time for the $+\frac{1}{2}\rightarrow-\frac{1}{2}$ transition of Gd^{3+} ions in tetragonal sites of CaF_2 can be fitted by

$$1/T_1=9.1\times10^2T^{1/2}+2.5\times10^{-4}T^5\ \text{sec}^{-1}. \quad (55)$$

It is obvious that the first term is not associated with the true spin-lattice relaxation time, but could be due to the cross relaxation with the neighboring lines since Gd^{3+} ions were also present in trigonal sites of the sample they used. Nevertheless, the last term agrees very well with our data.

IV. CONCLUSION

The theoretical estimates along with the experimental data for various relaxation rates for the cases considered in the last chapter are collected in Table III. It is seen that the measured relaxation rates agree reasonably well with the theoretical predictions considering the many approximations in the theory. Furthermore, the pronounced anisotropy in T_1 found experimentally for Sm^{3+} in LES and its agreement with the theoretical predictions support us to believe in the correctness of the theory. One is, therefore, confident that the combined Van Vleck–Orbach theory correctly describes the behaviors of the spin-lattice relaxation for the rare-earth ion at low temperatures.

It is interesting to note that from our experimental data and theoretical estimates for Tm^{2+}, Ho^{2+}, Yb^{3+}, and Sm^{3+} the matrix elements of the dynamic crystalline fields for these ions are $\sim10^3\ \text{cm}^{-1}$ which agree very well with the experimental results and theoretical calculations for some rare-earth ions in LES and double nitrates obtained by Scott and Jeffries.[10] This statement can be expressed as for Kramers salts,

$$\frac{1}{T_1}\sim10^{66}\sum_{p_t}\frac{g^2\beta^2H^4T}{\rho v^5{\Delta_{p_t}}^2}|\langle p_t|J_z|a\rangle|+10^{-3}\sum_{p_t}\frac{T^9}{\rho^2v^{10}{\Delta_{p_t}}^4}+10^{82}\sum_{p_t}\frac{{\Delta_{p_t}}^3}{\rho v^5}\exp\left(-\frac{\Delta_{p_t}}{kT}\right)\text{sec}^{-1}, \quad (56)$$

[41] R. Lacroix, Helv. Phys. Acta **30**, 374 (1957).
[42] R. Lacroix, Arch. Sci. (Geneva) **11**, 141 (1958).
[43] R. Lacroix, Proc. Phys. Soc. (London) **77**, 550 (1961).
[44] R. Bierig, M. Weber, and S. Warshaw, Phys. Rev. **134**, A1504 (1954).

in which the last term exists only when $\Delta_{p_t}<k\Theta_D$. For example, we shall apply this empirical formula for Nd^{3+} in YGaG and YAlG. Our measurements indicate Δ_{p_t} to be 85 and 75 cm^{-1} for YGaG and YAlG, respectively. Therefore, we obtain,

$$1/T_1\sim 10T+10^{12}\exp(-85\times 1.44/T)\ \text{sec}^{-1} \quad (57)$$

for YGaG, and

$$1/T_1\sim 10T+10^{11}\exp(-75\times 1.44/T)\ \text{sec}^{-1} \quad (58)$$

for YAlG. The last two equations agree remarkably well with the measurements, Eqs. (48) and (49).

Scott and Jeffries[11] have also reported that their experimental data for Nd^{3+} in LES agree very well with their theoretical calculations in which they have taken $p_n=1$, $n=2$, 4, 6. According to them the largest contribution comes from the $n=6$ terms. Consequently, there are uncertainties of an order of magnitude in the direct process and of three orders of magnitude in the two-phonon process. Because of these uncertainties in the Orbach's orbit-lattice interaction, we might as well use our empirical formula Eq. (56) which could serve to estimate the relaxation rate better than to two orders of magnitude.

In addition to the conventional processes, a new process predicted by Orbach and Blume, $T_1^{-1}\propto T^5$, has been observed for Eu^{2+} in CaF_2 in which the matrix element of the dynamic crystalline fields have been found to be $\sim$35 cm^{-1}. If we just consider that the relaxation is due to the modulation of the crystalline field, we will expect the matrix element of the dynamic crystalline field for Gd^{3+} in CaF_2, whose total crystalline field splitting is 0.1491 cm^{-1}, to be $\sim$30 cm^{-1}. Hence, we might guess the relaxation rate for Gd^{3+} in CaF_2 to be[45]

$$1/T_1\simeq 8T+2.6\times 10^{-4}T^5\ \text{sec}^{-1} \quad (59)$$

in which the last term is in exceptionally good agreement with the data measured by Bierig *et al.* The first term can be checked easily if a sample having all the Gd^{3+} ions present in a cubic site is used.

Above all, one may be surprised that theory and experiment for rare-earth ions at low temperatures agree so satisfactorily. The reasons are: J is a good quantum number; the crystals have been carefully prepared; the measurements were taken at the magnetic fields large compared to the linewidths; the lines at which the experiments were performed are well separated from the rest so that the complication of cross relaxation is avoided, and the orbit-lattice interaction is strong so that the impurities do not cause trouble.

ACKNOWLEDGMENTS

The author would like to express his indebtedness to Professor R. Orbach, Professor N. Bloembergen, Professor J. H. Van Vleck, Professor G. Seidel, and Professor R. V. Jones for their interest, encouragement, suggestions, and illuminating discussion during the whole course of this work. The kindness of W. P. Wolf, L. Rimai, Y. R. Shen, E. Sabisky, and F. Molea for supplying the crystals used in this work is also acknowledged.

[45] A. A. Manekov and Yu. E. Pol'skii, Zh. Eksperim. i Teor. Fiz. **45**, 1425 (1963) [English transl.: Soviet Phys.—JETP **18**, 985 (1964)] have found $T_1\sim$20 msec at 4.2°K. This is in reasonably good agreement with the first term in Eq. (59).